Analyst

Cite this: *Analyst*, 2012, **137**, 1252

www.rsc.org/analyst

PAPER

Development of molecularly imprinted polymer films used for detection of profenofos based on a quartz crystal microbalance sensor

Na Gao,†[a] Jianwei Dong,†[a] Ming Liu,[b] Baoan Ning,[b] Chaonan Cheng,[a] Chun Guo,[a] Caihong Zhou,[a] Yuan Peng,[b] Jialei Bai[b] and Zhixian Gao*[b]

Received 17th November 2011, Accepted 21st December 2011
DOI: 10.1039/c2an16120f

A quartz crystal microbalance (QCM) sensor based on molecularly imprinted ultra-thin films was developed for detecting profenofos in real samples. Films prepared by physical entrapment (MIP-A) and *in situ* self-assembly (MIP-B) were compared. The results indicated that the best sensing signal was obtained through the *in situ* self-assembly method. The QCM sensor chip was pretreated with 11-mercaptoundecanoic acid (MUA) to form a self-assembled monolayer (SAM), and then polymer films were immobilized directly on the SAM using surface-initiated radical polymerization. In this paper, all detection experiments were taken in air. The reaction was processed in solution, and the electrode was washed with deionized water and dried with N_2 before QCM measurement. The film was characterized by a scanning electron microscope (SEM), AC impedance and cyclic voltammetry. Analysis of the QCM response in the presence of different concentrations of profenofos showed a good linear correlation during 1.0×10^{-8} to 1.0×10^{-5} mg mL^{-1} ($y = 5\log x + 42.5$, $R = 0.9960$) and 1.0×10^{-5} to 1.0×10^{-3} mg mL^{-1} ($y = 25.86\log x + 146$, $R = 0.9959$), respectively. The MIP-QCM sensor was used to detect profenofos in tap water, and showed good recovery and repeatability.

1. Introduction

Profenofos, also known as *O*-(4-bromo-2-chlorophenyl)-*O*-ethyl-*S*-propyl phosphorothioate, is an extensively used organic phosphorus pesticide (OPP). In modern agriculture, the usage of OPPs has great importance in the control of harmful microorganisms and insects across the world. It has been estimated that about one-third of crop production would be lost without chemical substances.[1] OPPs are a class of pesticides that generally act as cholinesterase inhibitors and are used to control a broad range of pests of cotton, rice, tobacco, sorghum, sugarcane and vegetables.[2] A large number of OPPs are used around the world every year and their residues are found in surface water, soil, ground, food, *etc.* OPPs and their residues pose a serious problem for food security due to their toxicity to humans and animals.[3] Consequently selective and sensitive methods for the detection of OPPs in the environment and in agro-food products are essential.[4,5]

The current methods for qualitative and quantitative analysis of OPPs are mainly based on gas chromatography (GC),[6] high-performance liquid chromatography (HPLC),[7,8] and gas chromatography-mass spectrometry (GC-MS).[9] The advantages of these methods are that they are accurate and sensitive. However, they are laboratory-based, time-consuming, and require expensive instruments and high consumption of reagents. In addition, pre-concentration or extraction steps are required before analysis.[10] Immunological methods, such as enzyme-linked immunosorbent assay (ELISA), have also been used in OPP detection.[11] These methods offer high specificity, sensitivity, simplicity, and suitability for the analysis of a large number of samples within a short time period.[12] Nevertheless, the biological materials used in immunological methods are expensive and unstable. So the innovation of a simple and low-cost method for determination of OPPs is urgently required.

A quartz crystal microbalance (QCM) is a simple, portable, sensitive, and cost effective gravimetric sensor, that has been widely used in food safety, environment monitoring and veterinary diagnosis. For example, QCM biosensors have been used for detection of viruses,[13] nucleic acids,[14] proteins,[15] and small molecular chemicals such as drugs and pesticides.[16,17] In the past few decades, immunoassay techniques have been widely used for pesticide detection. However, biomolecules such as antibodies and nucleic acids are fragile and not readily available. These limitations have stimulated research and development of synthetic selective receptors that can mimic the recognition properties of these biomolecules which are stable.[18,19] With high stability, selectivity and analyte sensitivity, the newly developed molecularly imprinted polymers (MIPs) are becoming a hot research topic for development of artificial receptors.

[a]*College of Food Science and Technology, Huazhong Agricultural University, Wuhan, 430070, China*
[b]*Tianjin Key Laboratory of Risk Assessment and Control Technology for Environment and Food Safety, Institute of Health and Environment Medicine, Tianjin, 300050, China. E-mail: gaozhx@163.com; Fax: +86 22 84655183; Tel: +86 22 84655183*
† These authors contributed equally to this work.

Molecular imprinting is a promising technique for preparation of polymers with pre-designed recognition sites that are complementary to the template molecules in size, shape and functionary. Prior to polymerization, the template, functional monomer, cross-linker and initiator are mixed in solvent, followed by the copolymerization of these reagents. Then the recognition sites for templates are created in the three dimensional cross-linked polymers. After eluting the templates, recognition sites are left in the polymerized network. The synthesis of MIPs involves the formation of the monomer–template complexes through electrostatic interactions,[20] non-covalent interactions,[21] covalent interactions,[22] or metal ion coordination.[23] MIPs have the advantages of easy preparation, stability in harsh environments and low cost. Based on these advantages, MIPs have been widely used in capillary electrophoresis,[24,25] immunoassays,[26,27] chromatography separations and solid-phase extractions,[28–30] and biosensor applications.[31,32]

The combination of the molecular imprinting technique (MIT) with QCM has attracted more and more attention in recent years. So far, two different approaches have been developed to immobilize MIPs onto sensor transducers. The method of immobilizing pre-made MIP particles on a transducer by physical entrapment or chemical coupling has been frequently used,[33,34] and the preparation of imprinted polymer films directly on a transducer surface was researched as a developing method.[35–37] For the film, thickness is one of the main factors which affects detection sensitivity. This factor can be easily controlled by the *in situ* self-assembly method. In addition, this method only needs a small amount of analyte and can reduce the costs.

In recent years, MIP films of certain compounds have been accomplished and applied to QCM sensors. Our research team has constructed a MIP-QCM sensor (Li, *et al.*) and MIP-SPR sensor (Dong, *et al.*) for profenofos detection. Physical entrapment and *in situ* self-assembly were used to prepare MIP films in these two studies, respectively.[38,39] In this study, we constructed a MIP-QCM sensor using the *in situ* self-assembly method. Furthermore, comparison of these two methods (physical entrapment and *in situ* self-assembly) was performed. The films of MIP-B prepared by the *in situ* self-assembly method using surface-initiated thermal radical polymerization showed good sensitivity and repeatability. A scanning electron microscope (SEM) was used to identify morphology of the film. AC impedance and cyclic voltammetry were used to identify the quality of the MIP film on the QCM sensor. The selectivity and repeatability of the film were also evaluated, and the working conditions of the QCM sensing system established were optimized. The MIP-B film modified QCM sensor was then used to detect profenofos in real samples. In this paper, all detection experiments were taken in air. The reaction was processed in solution, and the electrode was washed with deionized water and dried with N_2 before QCM measurement.

2. Experimental

2.1. Materials and reagents

Methacrylic acid (MAA) was supplied by Acros Organics (New Jersey, USA). Profenofos, chlorpyrifos, parathion, dichlorvos and omethoate were obtained from the Dr. Ehrenstorfer Laboratories (Augsbury, Germany). 1-(3-Dimethylaminopropyl)-3-ethylcarbodiimide hydrochloride (EDC·HCl) and *N*-hydroxysuccinimide (NHS) were obtained from Aladdin (Shanghai, China). 11-Mercaptoundecanoic acid (MUA) and 2,2′-azobis(2-amidinopropane) hydrochloride (ABAH) were obtained from J&K Scientific Ltd (Europe). Trimethylopropane trimethacrylate (TRIM) was obtained from TCI (Shanghai, China). 2,2-Azobisiobutyronitrile (AIBN) was supplied by Aldrich (Milwaukee, WI, USA). Ethylene glycol dimethacrylate (EGDMA) was supplied by Sigma. All other chemicals were of analytical grade and obtained from Tianjin Chemical Co. Ltd (Tianjin, China).

The Britton–Robinson (B–R) buffer (pH 6.09) was used throughout the experiment.

2.2. Apparatus

The QCM obtained from Stanford Research Systems Inc (USA) is composed of a frequency counter, crystal holder, oscillator module, and PC interface connection for signal output visualization. The crystals were AT-cut 5 MHz specimens with gold-plated chips (331 μm thick and 1 inch in diameter). The exposed area of the front electrode in contact with the liquid is ~1.37 cm^2. The active electrode oscillation is mostly restricted to the area of overlap between the two circular pad chips or ~0.4 cm^2. The crystal is placed in the detection cell and clamped by two O-rings so that one side of the electrodes is exposed to the sample solution.

The Sauerbrey equation has been established for the AT-cut shear mode QCM, which relates the mass change per unit area at the QCM chip surface to the observed change in oscillation frequency of the crystal: $\Delta f = -C_f \cdot \Delta m$ where Δf = the observed frequency change in Hz, Δm = the change in mass per unit area in g cm^{-2}, C_f = the sensitivity factor for the crystal (56.6 Hz μg^{-1} cm^2 for a 5 MHz AT-cut quartz crystal at room temperature).

AC impedance and cyclic voltammograms of the QCM electrodes were measured in an electrochemical cell with a three-electrode system, which was consisted of a KCl saturated Ag/AgCl electrode as the reference electrode, a platinum electrode as the counter electrode, and a MIP-modified QCM electrode as the working electrode. The electrolyte solution consisted of 50 mM $K_3[Fe(CN)_6]$ and 1 M Na_2SO_4. The electrochemical measurements were carried out on an IviumStat electrochemical workstation (Netherlands).

2.3. Preparation of imprinted polymer thin film

2.3.1. Preparation of MIP-A. For the preparation of the polymer, profenofos (1 mmol) and MAA (4 mmol) were added to a 100 mL round-bottomed flask and dissolved in 60 mL acetonitrile for precipitation polymerization, and kept at 4 °C overnight. The cross-linker EGDMA (20 mmol) and the initiator AIBN (10 mg) were added. After being oscillated and purged with N_2 for 10 min to remove oxygen, the round-bottomed flask was sealed and kept in a thermostatic water bath (60 °C) for 24 h. The MIP-A particles were collected by centrifuging at 4000 rpm for 10 min. The template was extracted from these particles by repetitive washing with methanol–acetic acid solution (9 : 1, v/v) until the template molecule could not be detected by UV

(λ = 220 nm) in the extraction solvent. Then the obtained particles were washed with methanol several times until pH 7 was reached. The MIP-A particles were finally dried under vacuum.

Immobilizing the MIP-A on the sensor surface was carried out as follows. MIP-A (15.0 mg) was dissolved in tetrahydrofuran (THF, 5.0 mL) containing polyvinyl chloride (PVC, 5.0 mg). 10 μL of the above mixture was added to the center of the electrode and spun at 5000 rpm. After THF was evaporated at room temperature in air, a polymer film was immobilized onto the surface of the electrode.

2.3.2. Preparation of MIP-B. Prior to use, the chip was washed with 4 mL fresh "piranha" solution (1/3, 25% H_2O_2/75% H_2SO_4) for 3 min, followed by rinsing with copious distilled water and absolute ethanol sequentially, and then dried by nitrogen. The freshly cleaned chip was dipped into 20 mL 1 mM MUA–ethanol solution, and kept at room temperature overnight. The gold electrode was then washed with ethanol and deionized water to remove excess thiols, dried by nitrogen, and a stable SAM of thiols was formed on the gold surface. The carboxyl groups on the SAM were activated by 10 mL EDC (0.2 M) and NHS (0.05 M) aqueous solution for 1 h. The chip was then transferred into 10 mL 200 mM ABAH aqueous solution, and kept at room temperature for another 3 h. The initiator-covered chip was dried by nitrogen, and immediately dipped into pre-polymerization solution, which contains 27 μL profenofos (template), 94 μL MAA (function monomer), 225 μL TRIM (cross-linker) and 7 mL dimethyl sulfoxide (DMSO). The pre-polymerization solution was purged with nitrogen for 10 min, and then the container was covered and sealed with Vaseline. Polymerization was carried out at 60 °C for 18 h in a hot-air oven. After the polymerization process, the electrode was repeatedly immersed in methanol–acetic acid solution (9/1, v/v) with gentle shaking to remove the templates as well as other possible residual chemicals. Finally, the chip was dried by nitrogen after washing for at least 8 h in order to remove the templates completely. The non-imprinted polymer (NIP-B) film was prepared in the same way without profenofos. Fig. 1 shows the schematic representation for the synthesis of a MIP film on the Au surface of a QCM chip.

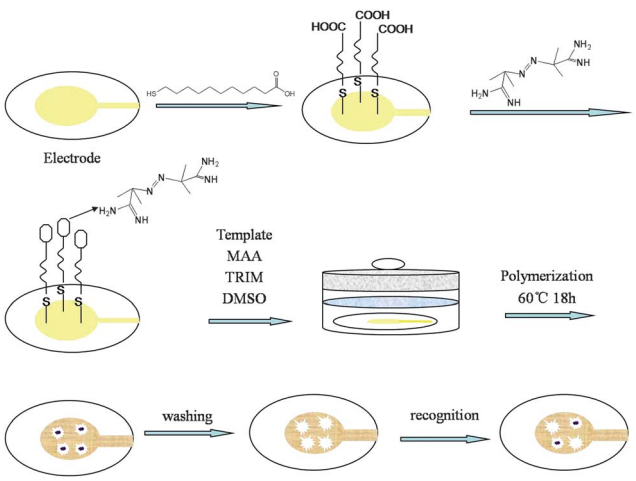

Fig. 1 Schematic representation for the synthesis of a MIP-B film on the Au surface of a QCM chip.

2.4. QCM measurement procedure

The measurement procedure was carried out as follows. Firstly, the MIP-coated electrode was put into a detection cell for several minutes to stabilize the QCM system. Secondly, the electrode was taken out and put into a series concentrations of standard solution to absorb templates into the recognition sites. Then the electrode was washed with deionized water and dried by nitrogen. Finally, the electrode was put back into detection cell, and the frequency shift for each solution was calculated ($\Delta F = f_i - f_0$) after stabilization. The detection conditions were maintained constantly throughout the experiment.

After each detection, the MIP-coated electrode was washed with methanol–acetic acid solution (9/1, v/v), methanol and deionized water sequentially for regeneration.

2.5. Selectivity measurement

The selectivity of the MIP-B film modified QCM was tested by measuring the signal responses of the MIP-B coated and NIP-B coated QCM sensor to profenofos and its analogues at a concentration level of 10^{-4} mg mL^{-1}. After each detection, the MIP-B and NIP-B coated electrodes were washed with methanol–acetic acid solution (9/1, v/v), methanol and deionized water sequentially for regeneration.

2.6. Sample preparation

The water sample was obtained from Heping District, Tianjin. Tap water (50 mL) was placed into a 100 mL centrifuge tube, and then spiked with 1×10^{-6}, 1×10^{-5}, and 1×10^{-4} mg mL^{-1} profenofos. Then, the spiked sample was placed in a 125 mL separatory funnel. Subsequently, 5 mL dichloromethane was added and extracted for 5 min by shaking. Extraction was repeated three times. The extracts were dehydrated by adding 1 g anhydrous sodium sulfate and then evaporated to near dryness in a rotary evaporator at 35 °C. The residue was re-dissolved in 10 mL B–R buffer (pH 6.09) and filtered using a 0.22 μm filter. Finally, the mixture was detected using the MIP-B QCM system.

3. Results and discussion

3.1. Sensor response

In this paper, all detection experiments were taken in air. Only 8–10 min was needed for the QCM system to reach a stable level.

To evaluate the molecular rebinding properties of the MIP film, a NIP film was also analyzed as reference under the same conditions. Fig. 2 shows the responses of MIP-A, MIP-B and NIP-B film coated QCM sensors to different concentrations of profenofos. The response of the MIP-B film coated QCM sensor increases significantly with the increment of profenofos concentration. In contrast, the response of the NIP-B film coated QCM sensor was very low, and showed a poorer linearity. The results indicated that MIP-B film afforded highly specific and strong signal response to the template molecule profenofos. For the MIP-B film, two different linear regions for profenofos solutions in the range of 1.0×10^{-8} to 1.0×10^{-5} mg mL^{-1} and 1.0×10^{-5} to 1.0×10^{-3} mg mL^{-1} were found, the linear regression equations were y (Hz) = 5log x (mg mL^{-1}) + 42.5 (R = 0.9960) and

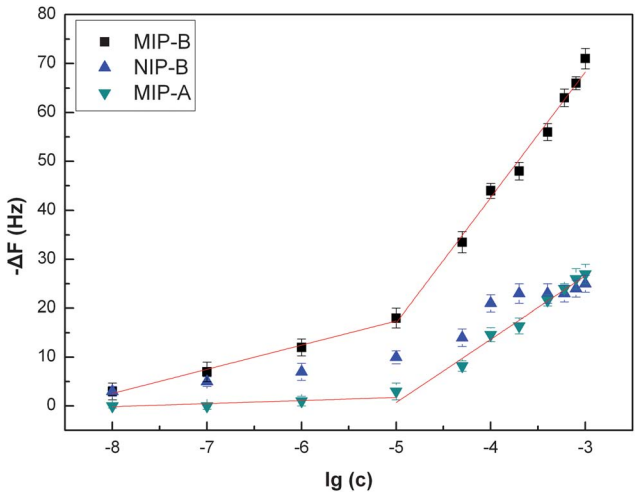

Fig. 2 The response of MIP-A, MIP-B and NIP-B film modified sensors to different concentrations of profenofos ($n = 3$).

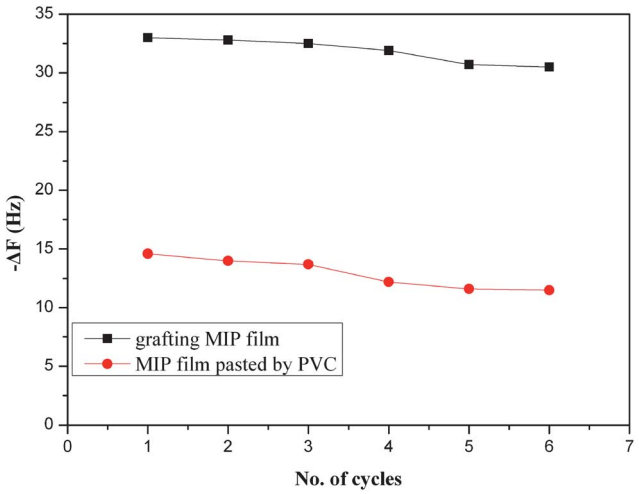

Fig. 3 Reproducibility of MIP-A (MIP film pasted by PVC) and MIP-B (grafting MIP film) modified QCM sensors at concentration levels of 1×10^{-4} mg mL^{-1}and 5×10^{-5} mg mL^{-1} respectively.

y (Hz) = 25.86log x (mg mL^{-1}) + 146 ($R = 0.9959$), respectively. It would be reasonable to assume that there are two kinds of rebinding sites existing in the MIP film; one is low rebinding sites, and the other is high rebinding sites. When the concentration of profenofos was at a low level, the high rebinding sites with a strong affinity to profenofos were occupied preferentially by template molecules. With increasing profenofos concentration, the low rebinding sites also become occupied. This result is similar to a previous report.[40] MIP-A showed same phenomenon as MIP-B, also having two different linear regions. However, the response signal of MIP-A was significantly lower than MIP-B, as well as having lower sensitivity. The resonant frequency of the crystal dropped, with 2547 Hz and 340 Hz after deposition of MIP-A and MIP-B respectively. According to the Sauerbrey equation, the change in mass per unit area of the MIP-A and MIP-B films were 45 μg cm^{-2} and 6 μg cm^{-2}, respectively. Assuming that the density of the growing film is 1.5 g cm^{-3},[41] the thickness of the MIP-A and MIP-B film was estimated to be approximate 300 nm and 40 nm. The thickness is one of the most important factors that influences the sensitivity of the MIP-coated sensor, and PVC may cover some recognition sites. This is why the response characteristic of MIP-B coated sensor was much better than that of MIP-A.

3.2. Reproducibility of the MIP film

The MIP film, as the recognition element of sensor, has the advantages of reproducibility and physical and chemical stability compared to bioelements. In this study, reproducibility of the MIP film was evaluated by measuring the same concentration of profenofos solution six times under the same conditions. After each assay, the MIP film was regenerated by sequential washes with methanol–acetic acid (9/1, v/v), methanol and deionized water. The results shown in Fig. 3 indicated that the response signal of both MIP-A and MIP-B films decreased with the increment of cycles. Response signals of MIP-A and MIP-B modified sensors had about 21% and 7.5% loss at the 6th cycle, respectively. As MIP-A particles were pasted by PVC, particles which were not firmly entrapped easily fell off the electrode surface, and as a result their stability was not good. If too much PVC was used, a large number of recognition sites would be covered. However, as MIP-B was grafted to the electrode by covalent bonding, the film would not fall off easily. The loss of the MIP-B film response signal was mainly due to incomplete washing of templates, and the decrease in response signal was slight enough to be tolerated; meaning that the MIP-B film sensor exhibited good reproducibility.

3.3. Surface characteristics of the MIP-B coated film

3.3.1. Surface observation of the MIP-B thin film. The surface of the QCM electrode was modified by MUA to form a SAM. Prior to polymerization, the initiator ABAH was covalently coupled to the carboxyl-terminated SAM. The amino groups of ABAH directed the interaction between the carboxyl of SAM and the imprinted polymer film. Using this method, we obtained the ultra-thin MIP-B film. Photo-polymerization was used in most of the researches reported[37,40–44] and special equipment is needed to avoid oxygen and to control temperature. In this study, thermal polymerization which is easy to operate and control was employed. The surface of the MIP-B film coated electrode and bare electrode was analyzed by SEM (Fig. 4). Comparing with the bare Au electrode (right), a uniform meshy layer was deposited on surface of the MIP-film coated electrode (left), which proves that the MIP-B film was synthesized on surface of the electrode.

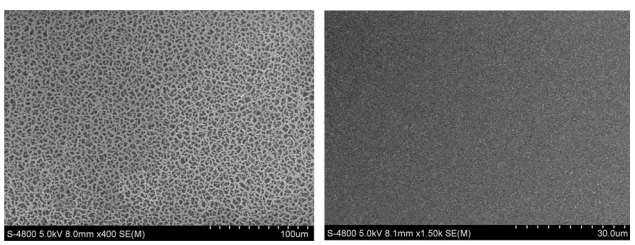

Fig. 4 SEM images of the surface of MIP-B film coated chip (left) and bare chip (right).

3.3.2. Characterization of the MIP-B coated QCM electrode. Fig. 5 shows cyclic voltammograms (CVs) of bare electrode and MIP-B film-modified electrode (prior to and after removal of the template profenofos) in 50 mM $K_3[Fe(CN)_6]$ probe solution (with 1 M Na_2SO_4). A couple of quasi-reversible redox peaks of the probe were obtained. The peak current of the "a" curve was higher than that of the "b" and "c" curves. This is because the non-conducting MIP-B film modified electrode blocked electron transfer of potassium ferricyanide. The "b" curve was higher than that of the "c" curve, indicating an increase in electron transfer after removal of profenofos molecules. This is likely because the recognition sites were left after removing the profenofos molecules, moreover, these recognition sites were connected to and touched the electrode surface. As a result potassium ferricyanide could diffuse to the electrode surface through these recognition sites.

AC impedance spectroscopy is an effective method to characterize a modified electrode surface. A classic AC impedance graph (Nyquist graph) comprises of an arc in the high frequency range and a line in the low frequency range. Fig. 6 shows the AC impedance spectra of a MIP-B film-modified electrode, before and after removal of template, and before and after interaction with different concentrations of profenofos in 50 mM $K_3[Fe(CN)_6]$ probe solution (with 1 M Na_2SO_4). Z' and Z'' represent the real impedance and imaginary impedance, respectively. Z' for "a" is about 8.5 KΩ, after removal of template profenofos, as seen in curve "d", Z' decreased to 3.4 KΩ. After interaction with 100 ng ml^{-1} and 500 ng ml^{-1} profenofos, Z' increased to 4 KΩ and 5 KΩ respectively. The change in resistance was attributed to the template profenofos, which inhibited electron transfer between the electrode and electrolyte. Before removal of the template, all recognition sites were occupied by profenofos, so the resistance is the largest. After removal of the template these recognition sites were left, so the conductivity of MIP film increased and the resistance decreased. After interaction with profenofos, some of recognition sites were occupied, so the resistance increased. The higher the concentration, the more recognition sites were occupied, which resulted in smaller conductivity and greater resistance.

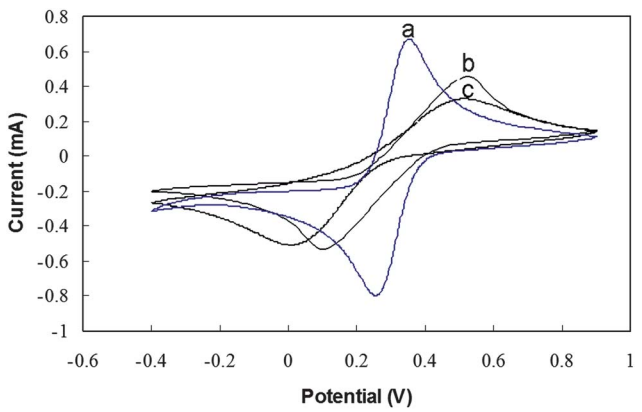

Fig. 5 CVs of bare electrode (a) and MIP-B film modified electrodes after (b) and before (c) removal of template profenofos in 50 mM $K_3[Fe(CN)_6]$ solution (with 1 M Na_2SO_4). The scan rate was 50 mV s^{-1}.

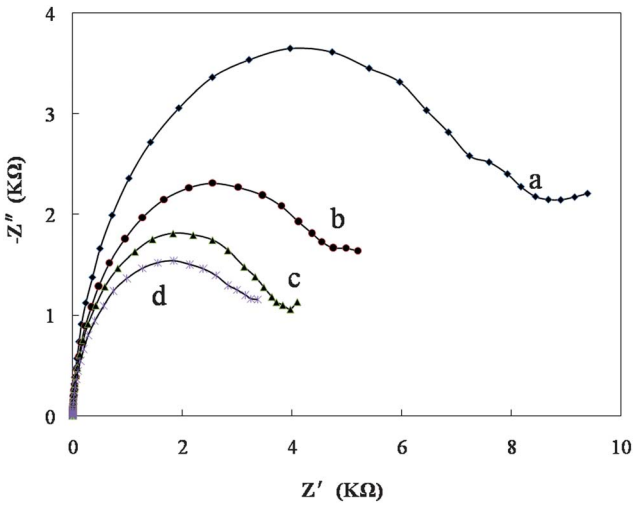

Fig. 6 AC impedance spectra of the MIP-B film modified electrode. (a) Before removal of template profenofos; (b) interaction with 500 ng mL^{-1} profenofos; (c) interaction with 100 ng mL^{-1} profenofos; (d) removal of template profenofos.

3.4. Selectivity of the MIP-B film sensor

The specificity is an important parameter for sensors. When a QCM sensor is used to detect targets in samples, it is inevitable that some structurally related compounds and other interferents of profenofos would affect the detection of profenofos. So in this study, analogues of profenofos such as chlorpyrifos and parathion as well as potential interferents such as dichlorvos and omethoate were selected to evaluate the selectivity of the MIP-B film coated QCM sensor.

Results shown in Fig. 7 indicate that no obvious interferences were detected by these compounds (structures shown in Fig. 8). Among the studied compounds, chlorpyrifos and parathion are most similar to profenofos in molecular shape and structure while dichlorvos and omethoate have similar functional groups

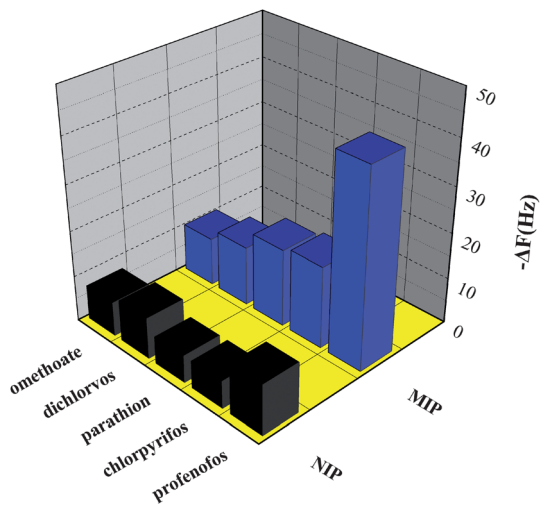

Fig. 7 The response of the MIP-B coated and NIP-B coated QCM sensor to profenofos and its analogues at concentration level of 10^{-4} mg mL^{-1}.

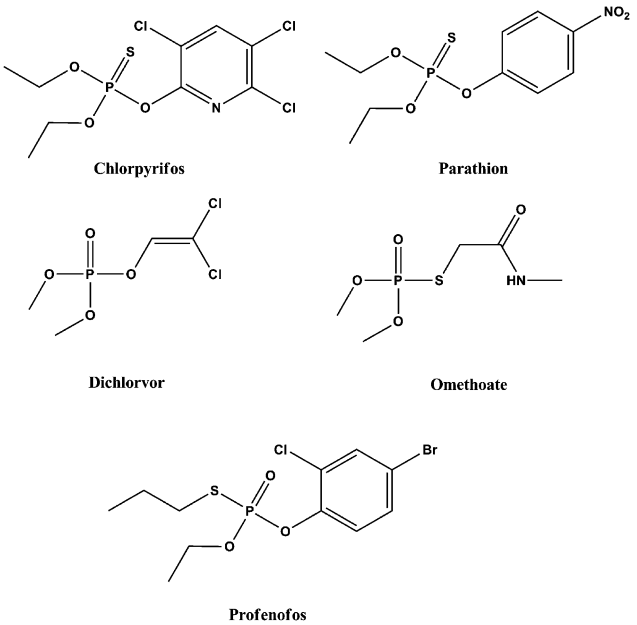

Fig. 8 Structures of the compounds used in the selectivity test.

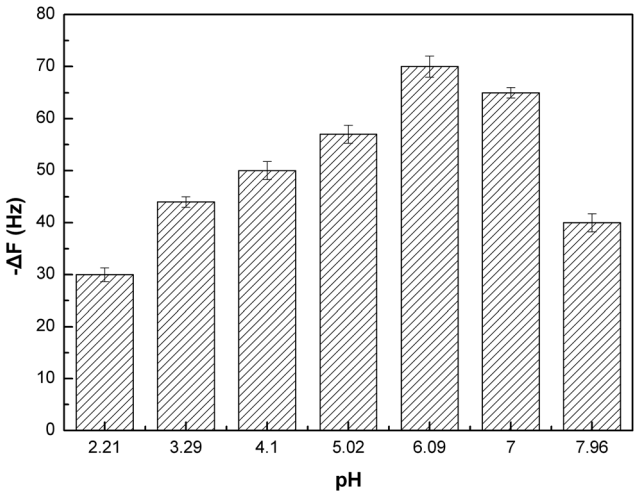

Fig. 9 The effect of pH on the frequency response at a concentration level of 1 mg mL^{-1} profenofos ($n = 3$).

to profenofos. Since molecular recognition was attributed to the specific shape and non-covalent interactions, chlorpyrifos and parathion show bigger responses than dichlorvos and omethoate. The results suggest that during the imprinting process the template created recognition sites which are complementary to the template in terms of size, shape and arrangement of the functional group. In contrast to the MIP-sensor, the NIP-sensor shows similar responses to all the studied pesticides. This result means that the NIP film does not have specific recognition sites because of the absence of templates. The above results strongly confirmed that a sensor with high selectivity for profenofos was obtained in our present study.

3.5. Optimization of buffer pH

Molecular imprinting is a method to prepare artificial antibodies. Recognition sites that are complementary to the templates in size, shape and functionary are created by copolymerization of functional monomer and cross-linker around the templates. In this study, MAA is used as the functional monomer with carboxyl functional groups. The rebinding between profenofos and MIP recognition sites are partly based on hydrogen bonds and other electrostatic forces. So the pH of buffer solution has an important effect on the response of the MIP film coated sensor to templates. Different pH vales of analyzing buffer were tested and optimized (Fig. 9). The maximum response is reached at a pH value of 6.09. As the pH value increased from 2.21 to 6.09 the responses increasing too, indicating that the adsorption of profenofos on the MIP-B film is increasing. However, when the pH increased from 6.09 to 7.96, the adsorption of profenofos on the MIP-B film decreased. Such a phenomenon is interpreted as follows. When the pH is less than 6.09, organic acid molecules and profenofos are both easily protonated. Consequently it is difficult for them to form hydrogen bonds with each other. Thus, adsorption of profenofos on the MIP-B film decreased. Moreover, many OPPs are easily hydrolyzed, especially in acidic or alkaline conditions. Hydrolysis products can not be absorbed because of the specificity of the MIP-B film. Profenofos is relatively stable at weak acidic and neutral conditions. So the maximum frequency response is reached at a pH value of 6.09.

3.6. Evaluation of the proposed method

To demonstrate the applicability of the coupled MIP-B QCM sensing method to profenofos detection in real samples, tap water was spiked with 1×10^{-6}, 1×10^{-5}, and 1×10^{-4} mg mL^{-1} profenofos. After the pre-processing described in "Section 2.6", the extracts were detected by the MIP-B QCM sensor. The results are shown in Table 1. The recoveries ranged from 94.87% to 97.43%, and the RSDs were less than 8%. Using a signal-to-noise ratio of 3 (S/N = 3), we calculated the detection limit to be 2.0×10^{-7} mg mL^{-1} for tap water. These results indicate that the developed method for the detection of profenofos residues in tap water offers a low detection limit, good accuracy, and repeatability.

4. Conclusions

Combining the advantages of the high selectivity of MIP and the high sensitivity of QCM sensors, a piezoelectric crystal sensor using ultra-thin molecular imprinting film as the recognition element has been developed. The ultra-thin film was prepared on the sensor chip directly by surface-initiated radical polymerization. The QCM sensor modified by ultra-thin film showed good reproducibility, wide linear range and good selectivity. The obtained sensor was used to detect spiked water samples, and the results showed satisfactory recoveries (94.87% to 97.43%), repeatability (RSD from 5.21% to 7.78%, $n = 3$), and detection limit (2.0×10^{-7} mg mL^{-1}, S/N = 3). This result demonstrates the feasibility of profenofos determination in tap water.

Table 1 Recovery of tap water spiked with profenofos ($n = 3$)[a]

Spiked concentration (mg mL^{-1})	Total spiked amount (mg)	Detected amount (mg)	Average recovery (%)	RSD[a] (%)
1×10^{-6}	5×10^{-5}	4.79×10^{-5}	95.93	7.78
1×10^{-5}	5×10^{-4}	4.74×10^{-4}	94.87	6.86
1×10^{-4}	5×10^{-4}	4.87×10^{-3}	97.43	5.21

[a] RSD = relative standard deviation.

Acknowledgements

This study was supported by National Natural Science Foundation of China (Grant Nos. 30972591 & 21107142) and Natural Science Foundation of Tianjin (Grant No. 11JCZDJC22400).

References

1 J. L. Tadeo, *Analysis of Pesticides in Food and Environmental Samples*, CRC Press, Boca Raton, 2008.
2 *The Pesticide Manual*, ed. C. D. S. Tomlin, British Crop Protection Council, Surrey, 11th edn., 1997.
3 P. Lea and F. Mladen, *Biosens. Bioelectron.*, 2003, **18**, 1–9.
4 J. R. Garbin, D. M. B. P. Milori, M. L. Simões, W. T. L. D. Silva and L. M. Neto, *Chemosphere*, 2007, **66**, 1692–1698.
5 E. J. Avramides, S. Gkatsos and J. Agric, *J. Agric. Food Chem.*, 2007, **55**, 561–565.
6 A. G. Frenich, M. J. Gonzalez-Rodrıguez, F. J. Arrebola and J. L. Martınez Vidal, *Anal. Chem.*, 2005, **77**, 4640–4648.
7 M. A. Rodriguez-Delgado and J. Hernandez-Borges, *J. Sep. Sci.*, 2007, **30**, 8–14.
8 F. Ahmadi, Y. Assadi, S. M. R. Milani-Hosseini and M. Rezaee, *J. Chromatogr., A*, 2006, **1101**, 307–312.
9 J. W. Wong, M. K. Hennessy, D. G. Hayward, A. J. Krynitsky, I. Cassias and F. J. Schenck, *J. Agric. Food Chem.*, 2007, **55**, 1117–1128.
10 J. L. Marty, D. Garcia and R. Rouillion, *TrAC, Trends Anal. Chem.*, 1995, **14**, 329–333.
11 G. S. Nunes, I. A. Toscano and D. Barceló, *TrAC, Trends Anal. Chem.*, 1998, **17**, 79–87.
12 K. Zeng, T. B. Yang, P. Zhong, S. Y. Zhou, L. Qu, J. He and Z. S. Jiang, *Food Chem.*, 2007, **102**, 1076–1082.
13 X. Su, S. F. Y. Li, W. Liu and J. K. Wang, *Analyst*, 2000, **125**, 725–730.
14 F. Kejun, L. Jishan, J. Jianhui, S. Guoli and Y. Ruqin, *Biosens. Bioelectron.*, 2007, **22**, 1651–1657.
15 G. Shen, H. Wang, S. Tan, J. Li, G. Shen and R. Yu, *Anal. Chim. Acta*, 2005, **540**, 279–284.
16 H. Sun and Y. S. Fung, *Anal. Chim. Acta*, 2006, **576**, 67–76.
17 N. Kim, I. S. Park and D. K. Kim, *Biosens. Bioelectron.*, 2007, **22**, 1593–1599.
18 F. Dickert, P. Lieberzeit and M. Tortschanoff, *Sens. Actuators, B*, 2000, **65**, 186–189.
19 K. Haupt and K. Mosbach, *Biochem. Soc. Trans.*, 1999, **27**, 344–350.
20 B. Sellergren and K. J. Shea, *J. Chromatogr., A*, 1993, **654**, 17–28.
21 D. A. Spivak and K. J. Shea, *Macromolecules*, 1998, **31**, 2160–2165.
22 M. J. Whitcombe, M. E. Rodriquez, P. Villar and E. N. Vulfson, *J. Am. Chem. Soc.*, 1995, **117**, 7105–7111.
23 R. Say, E. Birlik, A. Ersöz, F. Yılmaz, T. Gedikbey and A. Denizli, *Anal. Chim. Acta*, 2003, **480**, 251–258.
24 V. T. Remcho and Z. Tan, *Anal. Chem.*, 1999, **71**, 248A–255A.
25 C. Cacho, L. Schweitz, E. Turiel and C. Perez-Conde, *J. Chromatogr., A*, 2008, **1179**, 216–223.
26 N. Lavignac, C. J. Allender and K. R. Brain, *Anal. Chim. Acta*, 2004, **510**, 139–145.
27 J. S. Metcalf and G. A. Codd, *Chem. Res. Toxicol.*, 2003, **16**, 103–112.
28 J. Nicholls, I. A. Takeuchi, T. Mosbach and K. Karube, *Anal. Chim. Acta*, 1996, **335**, 71–77.
29 R. Say, A. Ersoz, H. Turk and A. Denizli, *Sep. Purif. Technol.*, 2004, **40**, 9–14.
30 M. A. Gore, R. N. Karmalkar and M. G. Kulkarni, *J. Chromatogr., B: Anal. Technol. Biomed. Life Sci.*, 2004, **804**, 211–221.
31 K. Taniwaki, A. Hyakutake, T. Aoki, M. Yoshikawa, M. D. Guiver and G. P. Robertson, *Anal. Chim. Acta*, 2003, **489**, 191–198.
32 R. Thoelen, R. Vansweevelt, J. Duchateau, F. Horemans, J. D'Haen, L. Lutsen, D. Vanderzande, M. Ameloot, M. vandeVen, T. J. Cleij and P. Wagner, *Biosens. Bioelectron.*, 2008, **23**, 913–918.
33 C. J. Percival, S. Stanley, A. Braithwaite, M. I. Newton and G. McHale, *Analyst*, 2002, **127**, 1024–1026.
34 B. S. Ebarvia, C. A. Binag and F. Sevilla III, *Anal. Bioanal. Chem.*, 2004, **378**, 1331–1337.
35 A. Kugimiya and T. Takeuchi, *Biosens. Bioelectron.*, 2001, **16**, 1059–1062.
36 C. J. Percival, S. Stanley, M. Galle, A. Braithwaite, M. I. Newton, G. McHale and W. Hayes, *Anal. Chem.*, 2001, **73**, 4225–4228.
37 M. Lotierzo, O. Y. F. Henry, S. Piletsky, I. Tothill, D. Cullen, M. Kania, B. Hock and A. F. P. Turner, *Biosens. Bioelectron.*, 2004, **20**, 145–152.
38 G. L. Li, W. Y, J. G. Han, Y. J. Fang and Z. X. Gao, *Chinese Journal of Analysis Laboratory*, 2009, **28**, 25–28.
39 J. W. Dong, N. Gao, Y. Peng, C. Guo, Z. Q. Lv, Y. Wang, C. H. Zhou, B. A. Ning, M. Liu and Z. X. Gao, *Food Control*, 2012, **25**, 543–549.
40 S. L. Yan, Y. J. Fang and Z. X. Gao, *Biosens. Bioelectron.*, 2007, **22**, 1087–1091.
41 V. Syritiski, J. Reut, A. Menaker, R. Gyurcsányi and A. Ö pik, *Electrochim. Acta*, 2008, **53**, 2729–2736.
42 T. Piacham, A. Josell, H. Arwin, V. Prachayasittikul and L. Ye, *Anal. Chim. Acta*, 2005, **536**, 191–196.
43 C. P. Wei, H. Q. Zhou and J. Zhou, *Talanta*, 2011, **83**, 1422–1427.
44 A. H. Wu and M. J. Syu, *Biosens. Bioelectron.*, 2006, **21**, 2345–2353.

